Investigating low and high load cycling tests as accelerated stress tests for proton exchange membrane water electrolysis

Li, Na; Araya, Samuel Simon; Kær, Søren Knudsen

Published in:
Electrochimica Acta

DOI (link to publication from Publisher):
10.1016/j.electacta.2021.137748

Publication date:
2021

Document Version
Accepted author manuscript, peer reviewed version

Investigating low and high load cycling tests as accelerated stress tests for proton exchange membrane water electrolysis

Na Li [a,*], Samuel Simon Araya [a], Søren Knudsen Kær [a]

[a] Aalborg University, Department of Energy Technology, Pontoppidanstræde 111, 9220 Aalborg Øst, Denmark

Abstract

In this paper, novel accelerated stress protocols have been proposed based on polarization and electrochemical impedance spectroscopy characterization conducted on three single cell assemblies: one for reference at constant load of 1 A cm $^{-2}$ and two dynamic loads consisting of a high load cycling between 1.2 A cm $^{-2}$ and 2 A cm $^{-2}$ and a low load cycling between 0 A cm $^{-2}$ (open circuit voltage) and 0.5 A cm $^{-2}$. Results showed that the degradation rate is 29.8 µV h $^{-1}$ for constant load test, 51.4 µV h $^{-1}$ for low load cycling test and -55.8 µV h $^{-1}$ for high load cycling test. Compared to the constant load operation, low load cycling operation could accelerate the cell performance decrease mainly due to cathode catalyst degradation. The high load cycling could lead to increased cell performance by reducing the ohmic resistance but degrades the anode catalyst significantly, which could compromise the cell's long-term stability. Besides, it is believed that this dynamic condition could accelerate the cell aging by accelerating the membrane thinning.

Keywords: Accelerated stress test, PEM water electrolyser, Load cycling, Hydrogen

1 Introduction

Due to the global energy and environmental problems caused by fossil fuel combustion, the development of clean and renewable energy sources such as wind and solar has become the focus of global research. Owing to the prominent advantages of quick response and wide dynamic operation range [1,2], proton exchange membrane (PEM) water electrolysis can utilize these fluctuating power sources as input to generate hydrogen through splitting water without emission of polluting gases into the environment [3,4]. Therefore, PEM water electrolysis has attracted much attention of researchers [5]. However, the balance of durability and cost of PEM water electrolyzer is one of the biggest challenges that hinders its commercialization [6,7].

The durability of PEM water electrolyzer is normally examined by investigating voltage increase via constant or dynamic current operation under specific temperature and pressure conditions [8–10]. Sun et al. [11] investigated the durability of a PEM electrolysis stack at a constant current density of 0.5 A cm $^{-2}$ for 7800 h and found that the cell performance decreased gradually with average degradation rate of 35.5 µV h $^{-1}$ per cell, which was due to the contamination of metallic impurities originated from the feed water. Long-term degradation test was also carried out by Christoph et al. [12], where a single cell test was operated at constant current density of 2 A cm $^{-2}$ for over 1000 h. They found significant cell degradation, which was attributed to the increased ohmic resistance caused by the passivation of Ti-PTL (porous transport layer) on anode. They also reported that cell current interruption could recover the cell performance.

It is worth noting that the traditional degradation test procedure of PEM water electrolyzer system and its components is time-consuming and expensive. Drawing lessons from the sister technology of fuel cell lifetime tests, accelerated stress tests (AST) are commonly used to shorten the degradation process using higher stress such as high current density, high temperature, high pressure, and load cycling etc., to accelerate cell ageing [13–15]. Among many of the AST protocols, load cycling is the most frequently used one. Weiß et al. [8] proposed an AST protocol in their test, where the cell was operated between high current density of 3 A cm $^{-2}$ and low current densities of 0.1 A cm $^{-2}$, combined with an open circuit voltage (OCV) test. The results showed that the cell performance was first increased but then decreased after prolonged cycling. Steffen et al. [16] carried out different current cycling modes between 0 - 2 A cm $^{-2}$ with different dwell times and compared them with constant load test at 2 A cm $^{-2}$. They showed that faster dynamic operation could improve the cell performance but cause more severe fluoride release from the membrane and catalyst binder and high gas crossover due to membrane thinning, and compared to constant load operation, the degradation rates of load cycling tests were lower. Similar results were also found by Christoph et al. [17], where they carried out single cell tests with different current density profiles consisting of constant and dynamic operations for 1009 h. They found that the high constant current density of 2 A cm $^{-2}$ led

* Corresponding author.

E-mail address: nal@et.aau.dk *(Na Li)*

to highest average degradation rate of 194 µV h^{-1}, no degradation was seen at the constant operation of 1 A cm^{-2}, and the dynamic operation could improve the cell performance as current switching could cause parts of performance recovery. In another study, a dynamic load profile between 0 to 2 A cm^{-2} was investigated, and it was found that the ohmic resistance of the cell decreased slightly at 60 ºC, which was attributed to the membrane thinning during the aging test [18]. It can be seen from the above investigations that both current values and the load cycling frequency affect cell performance.

Although some performance and durability studies of PEM water electrolysis have been carried out in literature, the degradation mechanisms have not been fully identified. It is still unclear which current density interval is mainly responsible for the single cell performance degradation. Besides, studies of the effects of dynamic operations under high load cycling (> 1 A cm^{-2}) on the durability of PEM water electrolysis are scarce. Therefore, in this study, novel AST proposals consisting of the current cycling of both high and low load cycling were employed to investigate different load cycling effects on the cell performance change. Two set of dynamic load cycling tests protocols are proposed and tested on separate single cell assemblies - one at high load current density range between 1.2 A cm^{-2} - 2 A cm^{-2} and another at low load current density range between 0 - 0.5 A cm^{-2} . A constant load operation of 1 A cm^{-2} was also carried out for comparison with the dynamic tests. The effect of the different dynamic operation protocols and the constant load on the single cell performance were investigated and degradation analysis was carried out.

2 Experimental

2.1 Membrane electrode assembly and test bench setup

The membrane electrode assembly (MEA) used in this test is a catalyst coated Nafion®117 membrane, where IrO_2 at a loading of 0.3 mg cm^{-2} was used as catalyst on anode side and Pt/C catalyst at loading of 0.5 mg cm^{-2} was used on the cathode side. For the porous transport layer (PTL), a carbon cloth covering on the outside of the catalyst was used as the cathode PTL and a 350 µm thick Ti felt, with a porosity of 81% and fiber diameter of 20 µm was used as the anode PTL. The active area of the MEA is 2.89 cm^2 (1.7 cm × 1,7 cm). The MEA was sandwiched between current collectors and end plates and fixed together with nuts and screws. By controlling the spring length on the screws, the compression pressure on the single cell was set to 2.61 MPa.

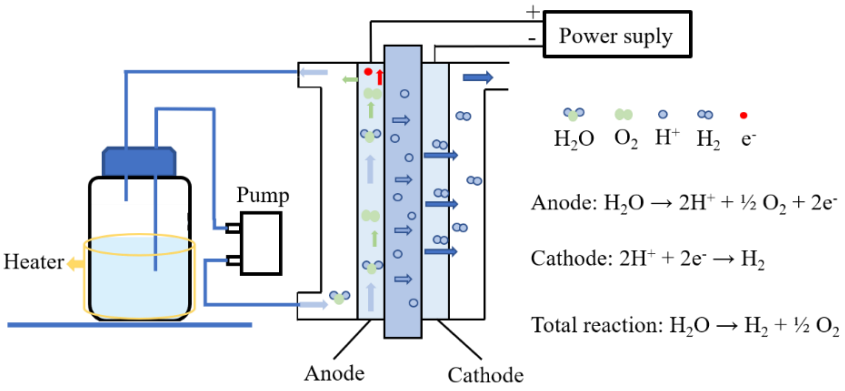

Fig. 1 The schematic of the single cell setup.

A schematic of the test bench used in this work can be seen in Fig. 1. The deionized (DI) water was circulated between the water tank and anode side of the single cell through a pump. The water flow rate in the system was 270 mL min^{-1}. A heater was employed to heat the water in the tank to keep a constant cell temperature. The power supply is a Gamry Reference 3000 potentiostat/galvanostat, which is connected to the anode (working electrode) and cathode (reference electrode) of the single cell. Oxygen produced on the anode side leaves the cell with the circulating water and is released into the air and the hydrogen produced on the cathode side is released to the fume hood.

2.2 Test procedure

Three single cell tests were carried out with different load profiles, which consist of constant and AST protocols as shown in Fig. 2. As can be seen in Fig. 2, the current density was set to 1 A cm^{-2} during the constant load test. For high load cycling teste, the current density was kept at 1.2 A cm^{-2} for 4 min and at 2 A cm^{-2} for 16 min in one cycle, and the cell was shut down for 10 min after every 10 hours operation. Likewise, for low load cycling test, the current density was kept at 0 A cm^{-2} for 4 min and at 0.5 A cm^{-2} for 16 min in one cycle, with 10 min break every 10 hours.

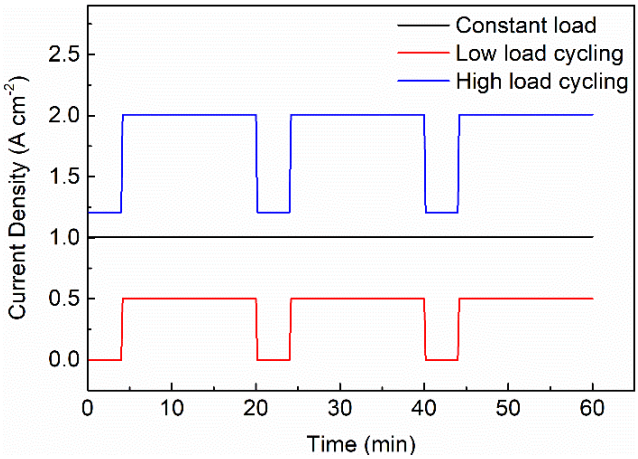

Fig. 2 Test protocols for durability test.

Before each test, the cell was operated for 72 h with DI water at 1 A cm $^{-2}$ and 60 ºC as a break-in step to activate the cell and remove the eventual metallic ions in the system. The test duration for each of the test was 350 h (1035 cycles for dynamic tests) and operating temperature was kept to 60 ºC for all the tests. Chandesris et al. [19], reported that the membrane degradation can be strongly increased when increasing the operation temperature from 40 ºC to 80 ºC. In the previous study of our group [16], it has been found that increase in the operating temperature (from 60 ºC to 90 ºC) has negative effect on the cell performance, where the cell has the smallest degradation rate at 60 ºC and the highest degradation rate at 90 ºC. Therefore, the operating temperature of 60 ºC was selected in this study to minimize the temperature effect on cell performance.

2.3 Characterization

Electrochemical characterization measurements were employed during each test to further understand the effect of operation modes on the cell performance. Electrochemical impedance spectroscopy (EIS) is a powerful tool, which can describe the composition of the total cell resistance loss including ohmic resistance, charge and mass transfer resistance separately [20]. Therefore, to better analyze the performance changes in this study both polarization curve and EIS measurements were carried out using the Gamry Reference 3000 potentiostat/galvanostat and booster. Polarization curves were recorded by varying the cell voltage from 1 V to 2.5 V. EIS spectra were recorded with the frequency range of 100000 Hz to 0.01 Hz, and 10 measurements points per decade for each step.

The obtained impedance data were fitted to the equivalent circuit (EC) model shown in Fig. 3, which consists of a pure resistor in series with three parallel R - CPE circuits. In Fig. 3, R_{ohm} represents the total ohmic resistance of components of the cell (membrane, catalyst layers, current collectors and other connectors in the test system). R_{HF}, R_{IF} and R_{LF} represent the high, intermediate and low frequency resistances, respectively and are connected in parallel with their respective constant phase elements (CPE), CPE_1, CPE_2, and CPE_3. The CPEs were employed to simulate the double layer capacitance, considering the non-uniform capacitance distribution and surface roughness of the single cell [21,22].

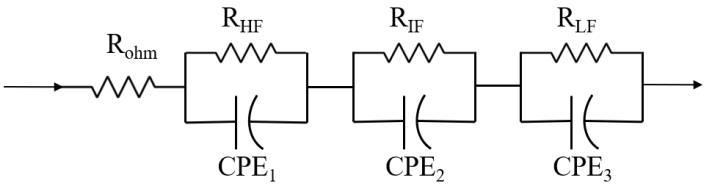

Fig. 3 Equivalent circuit for impedance spectra fitting, R_{ohm} represents the ohmic resistance, R_{HF} represents the high frequency resistance, R_{IF} represents the intermediate frequency resistance, R_{LF} represents the low frequency resistance, and the CPEs represent the corresponding constant phase elements.

3 Results and discussion

3.1 Cell performance change

The performance changes of the single cell under different test protocols are shown in Fig. 4. The average voltage degradation rates are 29.8 µV h $^{-1}$, 51.4 µV h $^{-1}$ and - 55.8 µV h $^{-1}$ for constant load test, low load cycling test and high load cycling test, respectively. The degradation rates of constant load and low load cycling are positive and the value of low load cycling is significantly higher than that of the constant load test, representing a more severe cell performance decrease for low load cycling test. However, the degradation rate during the high load cycling test is negative, which means that the cell performance increased during this dynamic test. Christoph et al. [17]carried out a similar dynamic operation (0 - 2 A cm $^{-2}$, interval of 10 min) in their tests, which lasted for 1009 h, their results

showed that the degradation rate of this dynamic test was 50 μV h^{-1}. The result of Christoph et al. is close to the degradation rate of the low load cycling test in this study, but the duration of 350 h in this study is shorter at almost one third. The effects of the two load cycling tests (0 - 0.5 A cm^{-2} and 1.2 - 2 A cm^{-2}) on cell performance and the corresponding degradation mechanisms are also analyzed through polarization curves and Nyquist plots in this study.

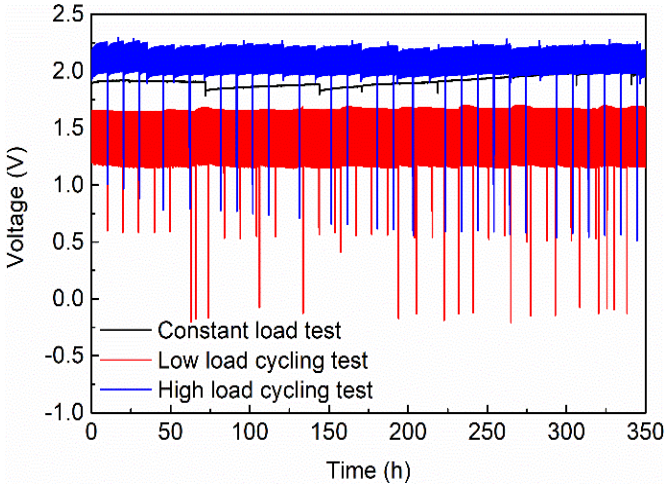

Fig. 4 Voltage change of each test throughout the entire test period.

3.2 Constant load operation (reference test)

In order to make a comparison with the dynamic tests, a single cell test was operated at a constant current density of 1 A cm^{-2} and operating temperature of 60 ºC for 350 h (equal to the duration of 1035 cycles of the dynamic tests). EIS and polarization curves were recorded every 72 h (equivalent to 207 cycles in dynamic test) during each test. The obtained results for constant load test are shown in Fig. 5.

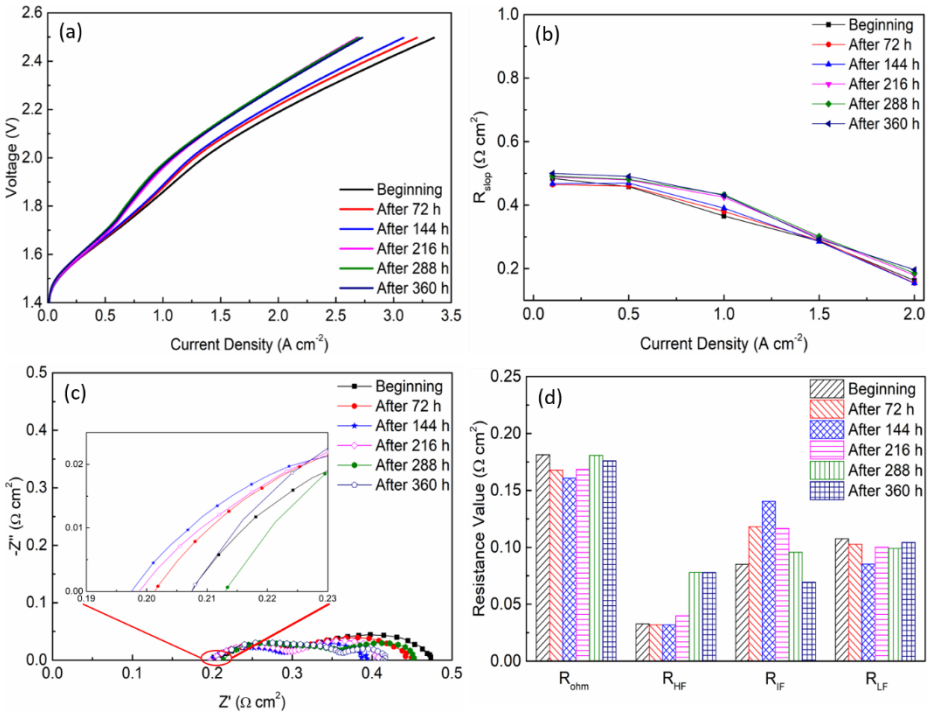

Fig. 5 Constant load test: (a) Polarization curves at different test points, (b) R_{slop} values, (c) EIS spectra and (d) resistance values.

As can be seen in Fig. 5 (a), the polarization curves are almost coincident at the constant load test when the current density is below 0.5 A cm^{-2}, which represents a stable cell performance. However, when the current density is above 0.5 A cm^{-2}, the cell voltage increased gradually and remained almost the same from the test point of 216 h until the end of the test. The polarization resistances (R_{slop}) were obtained by calculating the slopes of the polarization curves at different current density points according to the equation

of $R_{slop}= \Delta V/\Delta i$, where ΔV represents the voltage gradient and Δi is the current density gradient. The variation trends of R_{slop} at different test points are shown in Fig. 5 (b). As can be seen in Fig. 5 (b), the values of R_{slop} decreased with increasing current density. This could be due to the fact that higher current density leads to faster reaction kinetics of both electrodes and thus decreases the total resistance of the cell. The values of R_{slop} increased slightly at the end of the tests compared to the beginning, representing an overall decreased cell performance.

The Nyquist plots of EIS spectra of the constant load test are shown in Fig. **5** (c). The high frequency intercept on the real axis represents the ohmic resistance of the single cell, corresponding to the R_{ohm} value in the EC model. It can be seen that there are three semicircular arcs in each Nyquist plot, which are modelled by the three R - CPE circuits in the EC model. However, there is no clear consensus in literature regarding the contributions of the different components and processes in the electrolysis cell to the semi-circles in the Nyquist plot. Therefore, to avoid confusion, in the current work we refer to the different resistances according to the frequency ranges of the semi-circles as R_{HF}, R_{IF} and R_{LF} in decreasing frequency order. It is known that the kinetics of the hydrogen evolution reaction on the cathode side are much faster than the kinetics of the oxygen evolution reaction on the anode side, which means that the polarization resistance is mainly caused by the anode charge transfer process [20,21,23,24]. It is reported that the contribution of the cathode processes at high frequency is small especially with a high Pt loading of 0.5 mg cm^{-2} and increases with the decrease of Pt loading [25]. Therefore, the charge transfer resistance caused by cathode process is neglected in some references [26,27]. However, in this study, where the total Pt/C loading is 0.5 mg cm^{-2}, there is a clearly distinguishable high frequency semi-circle. Though this high frequency semi-circle may include charge transfer losses from both electrodes, it is suspected that it is dominated by the cathode side charge transfer losses [25,28]. Therefore, the diameter of the first semicircular arc at the high frequency is associated to the charge transfer resistance dominated by hydrogen evolution reaction, R_{HF} in the EC model and the diameter of the second semicircular arc in the intermediate frequency region is dominated by the charge transfer resistance dominated by oxygen evolution reaction, R_{IF} in the EC model. Lastly, the third semicircular arc at low frequency is dominated by the mass transfer process, corresponding to the value of R_{LF} in the EC model.

As can be seen in Fig. 5 (c), the high frequency intercept on the x-axis shifted to the left first during the first 144 h, then shifted to the right until 288 h and shifted to the left again after 350 h operation. The results of the fitted resistances are shown in Fig. 5 (d). As can be seen, the R_{ohm} values experienced a slight decrease first and then increased at the later stage, and the final value is almost the same as the initial one. The slight ohmic resistance decrease at the early stages of the test could be due to the membrane thinning phenomenon caused by the chemical attack, which is due to the fact that the catalyst dissolution and degradation may happen with time during the operation, and this could accelerate the generation of H_2O_2 and lead to chemical attack of the membrane [29,30]. It is reported that the Ti passivation becomes especially pronounced when the cell is operated at 1 A cm^{-2} intensively [31]. The ohmic resistance increase at the later stage could be due to the oxidation of the Ti anode transport layer, which could lead to increased contact resistance at the interface of the MEA [32]. In this study, these two effects cancel each other out for what concerns the ohmic resistance. However, the oxidation of Ti seems to contribute more than the membrane thinning to the cell performance, as can be seen from the overall cell performance decrease during the test. Moreover, both effects will contribute negatively to the cell's durability if not mitigated.

The R_{HF} values were rather small and remained almost unaltered before 216 h test but then increased significantly from this test point to the end of the test. This could be due to the fact that the cathode charge transfer resistance is negligible for a new single cell due to the fast reaction kinetics of the hydrogen evolution reaction [26,33]. However, the cathode catalyst may dissolve or be corroded during the test which may have led to decreased catalytic activity and an increase in the cathode charge transfer resistance. Besides, as reported by Christoph et al. [12], Ti dissolution could occur during the oxygen evolution and the Ti species were found in the cathode area of the cell acting as contaminants, which could lead to reduced cathode performance.

The values of R_{IF} values increased first from 0.085 Ω cm^2 to 0.14 Ω cm^2 at 144 h and then decreased to 0.07 Ω cm^2 at the end. The R_{IF} values are higher than the R_{HF} values, which indicates that the anode charge transfer loss is more responsible for the polarization losses in the Nyquist plot. The changes of R_{LF} values are not regular but the changes are small and the value at the end is close to the initial value of the test. This shows that mass transport is not an issue under constant load operation. However, it is worth noting that a very high-water flow rate of 270 mL min^{-1} has been used for all the tests, which represents a rather high over-stoichiometry. Therefore, the contribution of mass transfer process is minimized for both constant load test and load cycling tests in this study.

3.3 Low load cycling operation

The performance variation of the low load cycling tests was investigated by the analysis of the polarization curves and EIS measurements recorded at different test points during this test. As can be seen in Fig. 6 (a), the cell performance decreased progressively during the whole duration of the test with increasing number of cycles. The polarization slopes in Fig. 6 (b) confirm this result, where the R_{slop} values increased with time at each test point.

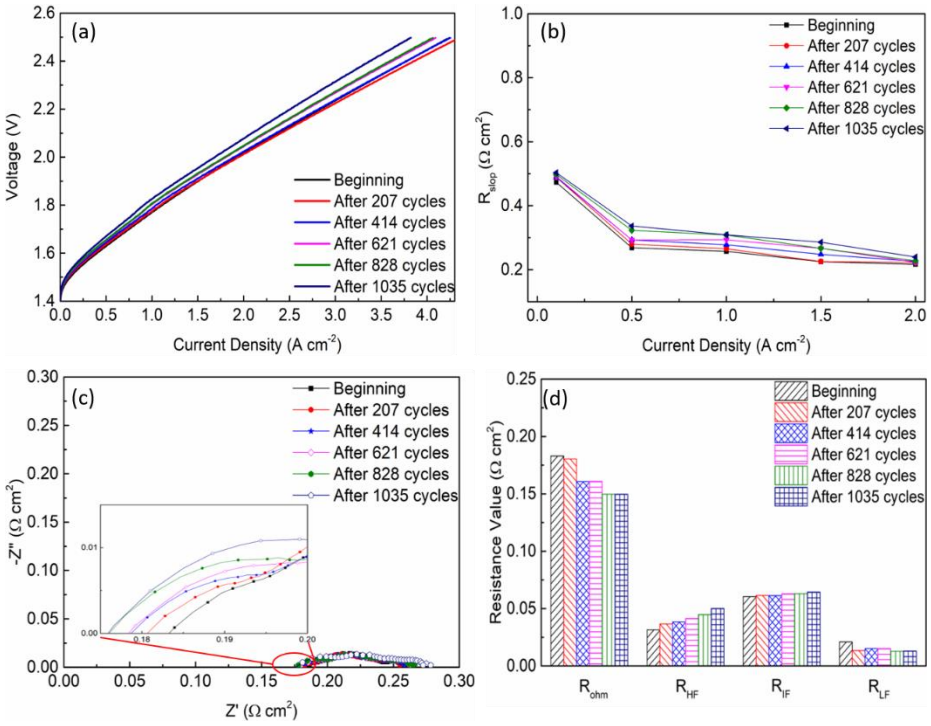

Fig. 6 Low load cycling test: (a) Polarization curves at different test points, (b) R_{slop} values, (c) EIS spectra and (d) resistance values.

The EIS data of the low load cycling test are presented in Fig. 6 (c). It can be seen that the high frequency intercept on the real axis gradually shifted to the left during the operation, implying that the dynamic test of low load cycling may improve the membrane conductivity to a certain extent by reducing the ohmic resistance. Three semicircular arcs can be seen in the Nyquist plots, but the changes in their diameters cannot be clearly seen in Fig. 6 (c). To explore this more the corresponding resistance values obtained by fitting the EIS data to the EC model are presented in Fig. 6 (d).

As can be seen in Fig. 6 (d), The ohmic resistance decreased gradually during the test (from 0.18 Ω cm ^{2} to 0.15 Ω cm ^{2}). Compared to the ohmic resistance increase of the constant load operation (from 0.19 Ω cm ^{2} to 0.20 Ω cm ^{2}), this dynamic test accelerated the ohmic resistance decrease. Chandesris et al. [19] reported that the peroxide concentration is high at low current density, which will produce chemical radicals that can attack the membrane. Therefore, the ohmic resistance decrease could be due to membrane thinning or catalyst layer thinning caused by radicals' attack.

The R_{HF} values increased linearly during the test. This low load cycling test, of which the current density was varied between 0 and 0.5 A cm $^{-2}$, consists of an open circuit step, which will lead to corrosion of the carbon cloth and Pt dissolution on the cathode side [18,34]. Besides, the load cycling may also cause cathode catalyst layer degradation and Pt agglomeration on the cathode, which will decrease the active area of the cathode catalyst [35]. This could all affect the hydrogen evolution reaction on the cathode side and lead to increased R_{HF} value. The R_{IF} values remain almost unaltered during the test with slight linear increasing tendency, which illustrates that the effect of the load cycling on the anode side can be said negligible.

The R_{LF} value decreased for the first step and then remained the same during the duration of the test. The values of the mass transfer resistances were rather small and the voltage changes due to the change in low frequency resistance in this low current density and open circuit current cycling are insignificant. Therefore, the main reason for the performance change in this test should be attributed to charge transfer losses, especially on the hydrogen side, which was also reported both in electrolysis and fuel cell studies [18,36–38]. It seems that the increase in R_{HF} counts more than the visible decrease in ohmic resistance, which by making the hydrogen evolution reaction more sluggish contributes to a decrease in the overall cell performance.

3.4 High load cycling operation

The effect of high load cycling test on the single cell performance is shown in Fig. 7. As can be seen in Fig. 7 (a), the polarization curves do not exhibit significant changes. Slight decrease in performance is seen below 1 A cm $^{-2}$, while an increase in performance is seen above 1 A cm $^{-2}$. It can be seen in Fig. 7 (b) that the values of R_{slop} decreased with increasing current density, this is because higher current density could lead to faster reaction kinetics of both electrodes and thus decrease the total resistance of the cell [39]. Different from the increase in R_{slop} with time both at constant load and low load cycling tests, the values of R_{slop} in this test increased slightly at low current density but decreased at high current density, which is consistent with the cell performance change in Fig. 7 (a). As Caroline

et al. [18] reported that the voltage change in the polarization curves at lower current density is mainly due to the charge transfer resistance, while the voltage change at higher current density is dominated by the ohmic resistance. Therefore, it is believed that the charge transfer resistance increased while the ohmic resistance decreased during the test. These changes are more clearly visible in the Nyquist plots and the fitted resistances in Fig. 7 (c) and (d), which are further explained below.

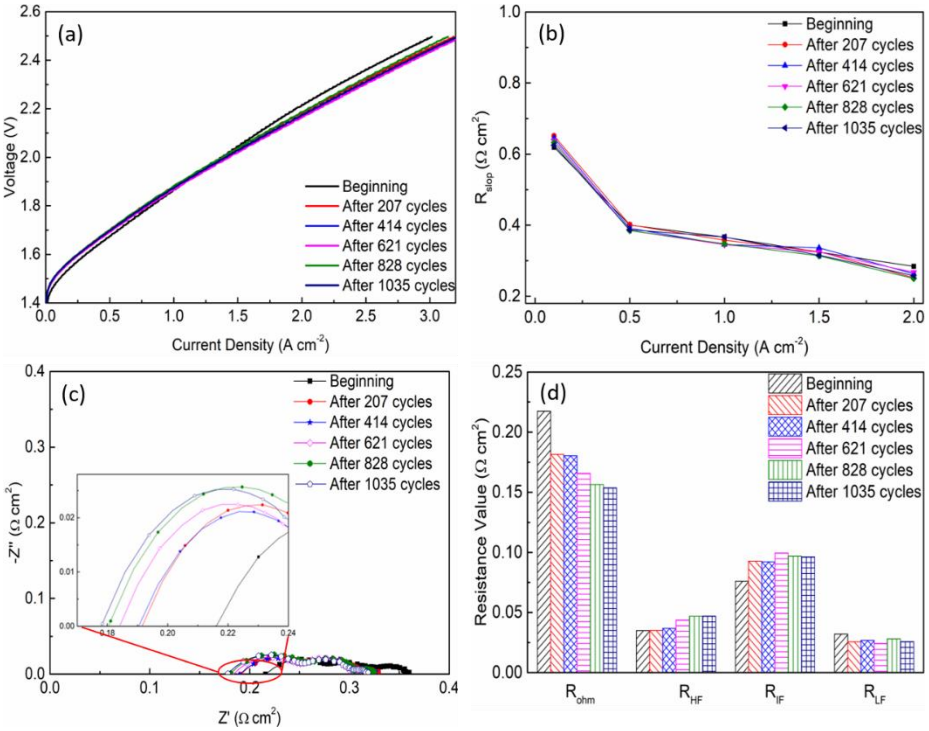

Fig. 7 High load cycling test: (a) Polarization curves at different test points, (b) R_{slop} values, (c) EIS spectra and (d) resistance values.

The EIS measurements for the high load cycling operation in Fig. 7 (c) show three semicircular arcs. The high frequency intercept on the real axis continued to shift to the left with increasing number of cycles during the test. The resistance values obtained by fitting the EIS plots to the EC model are presented in Fig. 7 (d). As can be seen, the R_{ohm} values decreased greatly after 207 cycles operation and kept decreasing during the remainder of the cycling test. After test duration equivalent to 207 cycles (72 hours), the high load cycling test showed significant decrease in ohmic resistance of - 36 mΩ cm^2 compared to the former two tests, which were + 4 mΩ cm^2 and - 3 Ω cm^2 for constant load and low load cycling, respectively. This large ohmic resistance decrease could be due to the membrane thinning, which could increase the ionic conductivity of the membrane [32]. Therefore, the results show that high load cycling operation could increase the cell performance by accelerating the membrane thinning phenomenon. However, this is not desirable. Although the membrane thinning could increase the cell performance to some extent, with time the membrane thinning could lead to gas crossover phenomenon and the risk of hot spots on the membrane, which will severely degrade the cell performance and even cause cell failure with time [19,35].

The R_{HF} value increased slightly during the duration of the test. The variations of R_{IF} and R_{LF} value are not consistent but an overall increase for R_{IF} and decreased for R_{LF} during the test are seen. Higher current density could lead to the gas crossover phenomenon accelerating the corrosion of carbon and passivation of Pt on the cathode side [17], which contribute to the increase in R_{HF} values in Fig. **7** (d). The value of R_{IF} increased significantly after 207 cycles and kept increasing during the cycling, this is to be expected as high current density operation could degrade the anode catalyst greatly during the tests [9,35]. Besides, as mentioned in the reference test, the Ti dissolution may happen when the current density reaches 1 A cm^{-2}, and the Ti species transfer from anode to cathode as contaminants will affect both the anode and the cathode performances. Furthermore, the R_{LF} during the cycling are lower than that of constant load test. This could be due to the current interruption (10 min break every 10 hours), which has a positive effect on the cell performance [17]. This break can give time for the gases in the channel to release and thus reduce the mass transfer resistance in the cell. It should be noted that both of the cycling tests (high load cycling and low load cycling) have lower R_{LF} values compared to the constant load test. This could be due to the current cycling making it easier for the evolved gases to be removed out of the cell. Considering the high over-stoichiometry of the feed water flow, the contributions of the R_{LF} values are not significant in both of the load cycling tests.

When comparing the fitted resistances in Fig.7 (d), it can be seen that R_{ohm} is the only resistance that decreases significantly while R_{HF} and R_{IF} both increase consistently and R_{LF} remains almost unaltered. Therefore, since the overall cell performance increases for

the high load cycling test despite the increase in both charge transfer resistances, it can only be attributed to the decrease in R_{ohm}, which according to fluoride emission results in [16] should be related to membrane thinning. Moreover, membrane thinning can exacerbate itself as more thinning can lead to more gas crossover, especially oxygen on the cathode Pt catalyst that will result in more H_2O_2 formation and attack the membrane [40].

3.5 AST effect analysis

Generally used AST protocols in PEM water electrolysis are high current density and dynamic load cycling [35]. As listed in Table 1, there have been some studies that investigated the performance change and components degradation mechanisms using AST protocols. As can be seen, high current density could lead to anode catalyst degradation while dynamic load cycling could lead to not only catalyst degradation but also membrane thinning and Ti-PTL passivation.

In this study, the effects of low and high dynamic load cycling AST protocols on the cell performance are investigated separately and they exhibit different degradation mechanisms. For low load cycling test, the charge transfer losses are dominant in the cell performance. The performance change is consistent with the variation trend of the charge transfer resistance (the total of R_{HF} and R_{IF} values variation in Fig. 6 (d)), which is associated with the catalyst layers degradation, especially on the cathode side. However, for high load cycling test, the changes in the ohmic resistance are more dominant. Although the charge transfer resistance increased during the cycling test, in this case the total decrease in the ohmic resistance was large enough to offset the losses and even increase the performance of the cell compared to the beginning of test. The significant ohmic resistance decrease indicates the thinning of the membrane.

Stressor	AST strategy	Failure mode	Reference
High current density	4 A cm $^{-2}$ for more than 750 h	Anode catalyst degradation (Ir leaches out)	[9]
Dynamic load cycling	0 A cm $^{-2}$ - 2A cm $^{-2}$, dwell time of 100 s, 60 s and 10 s for each test	Fluoride emission with fast load switches	[16]
OCV-AST (dynamic load cycling)	3 A cm $^{-2}$ for about 10 min, 0.1 A cm $^{-2}$ for about 10 min and an OCV for about 10 min	Passivation of Ti-PTL and hydrous iridium oxide	[8]
On/off (dynamic load cycling)	0 – 1 A cm $^{-2}$ for 5500 h	Catalyst layer corrosion and membrane thinning	[30]
Low load cycling	0 A cm $^{-2}$ – 0.5 A cm $^{-2}$	Charge transfer losses especially on the hydrogen side	Current work
High load cycling	1.2 A cm $^{-2}$ – 2 A cm $^{-2}$	Membrane thinning and catalyst degradation	Current work

Table 1 Examples of AST strategies used in PEM water electrolysis

Although the degradation mechanisms obtained in this study are consistent with that of the examples in Table 1, it is difficult to compare different experiment results which come from different laboratories with different operating conditions and test benches. When comparing the obtained degradation rates of the constant load reference operation in this work with the proposed AST tests, a significant saving in the test duration and cost can be achieved as low load cycling cause almost doubles the degradation rate and both dynamic operations cause membrane thinning. However, it is not possible to conclude on the acceleration factor of both the AST tests as it is not known when the membrane thinning in the current work would result in significant performance decrease or cell failure.

4 Conclusion

Novel accelerated stress protocols (dynamic load of 0 – 0.5 A cm $^{-2}$ and 1.2 A cm $^{-2}$ – 2 A cm $^{-2}$) were provided in this study. The effects of the accelerated stress tests on the cell performance were investigated and a constant load test at 1 A cm $^{-2}$ was also carried out as a reference test. EIS and polarization curves were recorded during each test to better describe the cell performance change. Results show that the low load cycling test could accelerate the cell performance decay, the mean voltage degradation rate of this operation is 51.4 μV h $^{-1}$, which is higher than the mean voltage degradation rate of constant load test (29.8 μV h $^{-1}$). The average voltage degradation rate of the high load cycling test is – 55.8 μV h $^{-1}$, which represents an increase in cell performance.

Compared to the normal prolonged degradation tests (usually more than 1000 h), which will lead to high costs, the dynamic tests in this study not only shortened the test period but also investigated both high and low load cycling effects on the cell performance, which better analyzed the effects of different current density intervals. It was found that the low current cycling contributes more to the voltage degradation and the ohmic resistance decreases significantly during the high load cycling, which could imply membrane thinning that could eventually lead to membrane failure. These trends can be compared to the degradation rates under constant load conditions and to the membrane thickness in the beginning to obtain acceleration factors, which can be used for lifetime prediction, provided that the limits of the membrane thinning are known, i.e., when the membrane thinning will lead to pin-hole formation and cell failure. In addition, the results of these tests can be used in load balancing application of electrolyzer systems, where load cycling profiles like the ones used in the current work can be used to mimic the fluctuations of renewable energy sources, such as solar and wind energy.

Acknowledgments

This work was supported by the Innovation Fund Denmark through the e-STORE project (Grant No. 4106-00025B). Na Li appreciates the financial support from China Scholarship Council.

Reference

[1] M. Carmo, D.L. Fritz, J. Mergel, D. Stolten, A comprehensive review on PEM water electrolysis, International Journal of Hydrogen Energy. 38 (2013) 4901–4934. https://doi.org/10.1016/j.ijhydene.2013.01.151.

[2] Q. Feng, X. Yuan, G. Liu, B. Wei, Z. Zhang, H. Li, H. Wang, A review of proton exchange membrane water electrolysis on degradation mechanisms and mitigation strategies, Journal of Power Sources. 366 (2017) 33–55. https://doi.org/10.1016/j.jpowsour.2017.09.006.

[3] S. Shiva Kumar, V. Himabindu, Hydrogen production by PEM water electrolysis – A review, Materials Science for Energy Technologies. 2 (2019) 442–454. https://doi.org/10.1016/J.MSET.2019.03.002.

[4] F. Barbir, PEM electrolysis for production of hydrogen from renewable energy sources, Solar Energy. 78 (2005) 661–669. https://doi.org/10.1016/j.solener.2004.09.003.

[5] A.S. Aricò, S. Siracusano, N. Briguglio, V. Baglio, A. di Blasi, V. Antonucci, Polymer electrolyte membrane water electrolysis: Status of technologies and potential applications in combination with renewable power sources, Journal of Applied Electrochemistry. 43 (2013) 107–118. https://doi.org/10.1007/s10800-012-0490-5.

[6] M. David, C. Ocampo-Martínez, R. Sánchez-Peña, Advances in alkaline water electrolyzers: A review, Journal of Energy Storage. 23 (2019) 392–403. https://doi.org/10.1016/J.EST.2019.03.001.

[7] M. Chandesris, R. Vincent, L. Guetaz, J.S. Roch, D. Thoby, M. Quinaud, Membrane degradation in PEM fuel cells: From experimental results to semi-empirical degradation laws, International Journal of Hydrogen Energy. 42 (2017) 8139–8149. https://doi.org/10.1016/j.ijhydene.2017.02.116.

[8] A. Weiß, A. Siebel, M. Bernt, T.-H. Shen, V. Tileli, H.A. Gasteiger, Impact of Intermittent Operation on Lifetime and Performance of a PEM Water Electrolyzer, Journal of The Electrochemical Society. 166 (2019) F487–F497. https://doi.org/10.1149/2.0421908jes.

[9] P. Lettenmeier, R. Wang, R. Abouatallah, S. Helmly, T. Morawietz, R. Hiesgen, S. Kolb, F. Burggraf, J. Kallo, A.S. Gago, K.A. Friedrich, Durable Membrane Electrode Assemblies for Proton Exchange Membrane Electrolyzer Systems Operating at High Current Densities, Electrochimica Acta. 210 (2016) 502–511. https://doi.org/10.1016/j.electacta.2016.04.164.

[10] A.S. Gago, J. Bürkle, P. Lettenmeier, T. Morawietz, M. Handl, R. Hiesgen, F. Burggraf, P.A. Valles Beltran, K.A. Friedrich, Degradation of Proton Exchange Membrane (PEM) Electrolysis: The Influence of Current Density, ECS Transactions. 86 (2018) 695–700. https://doi.org/10.1149/08613.0695ecst.

[11] S. Sun, Z. Shao, H. Yu, G. Li, B. Yi, Investigations on degradation of the long-term proton exchange membrane water electrolysis stack, Journal of Power Sources. 267 (2014) 515–520. https://doi.org/10.1016/j.jpowsour.2014.05.117.

[12] C. Rakousky, U. Reimer, K. Wippermann, M. Carmo, W. Lueke, D. Stolten, An analysis of degradation phenomena in polymer electrolyte membrane water electrolysis, Journal of Power Sources. 326 (2016) 120–128. https://doi.org/10.1016/j.jpowsour.2016.06.082.

[13] R. Petrone, D. Hissel, M.C. Péra, D. Chamagne, R. Gouriveau, Accelerated stress test procedures for PEM fuel cells under actual load constraints: State-of-art and proposals, International Journal of Hydrogen Energy. 40 (2015) 12489–12505. https://doi.org/10.1016/j.ijhydene.2015.07.026.

[14] S. Zhang, X. Yuan, H. Wang, W. Mérida, H. Zhu, J. Shen, S. Wu, J. Zhang, A review of accelerated stress tests of MEA durability in PEM fuel cells, International Journal of Hydrogen Energy. 34 (2009) 388–404. https://doi.org/10.1016/j.ijhydene.2008.10.012.

[15] Y. Jeon, S.M. Juon, H. Hwang, J. Park, Y.G. Shul, Accelerated life-time tests including different load cycling protocols for high temperature polymer electrolyte membrane fuel cells, Electrochimica Acta. 148 (2014) 15–25. https://doi.org/10.1016/j.electacta.2014.10.025.

[16] S.H. Frensch, F. Fouda-Onana, G. Serre, D. Thoby, S.S. Araya, S.K. Kær, Influence of the operation mode on PEM water electrolysis degradation, International Journal of Hydrogen Energy. 44 (2019) 29889–29898. https://doi.org/10.1016/j.ijhydene.2019.09.169.

[17] C. Rakousky, U. Reimer, K. Wippermann, S. Kuhri, M. Carmo, W. Lueke, D. Stolten, Polymer electrolyte membrane water electrolysis: Restraining degradation in the presence of fluctuating power, Journal of Power Sources. 342 (2017) 38–47. https://doi.org/10.1016/J.JPOWSOUR.2016.11.118.

[18] C. Rozain, E. Mayousse, N. Guillet, P. Millet, Influence of iridium oxide loadings on the performance of PEM water electrolysis cells: Part II – Advanced oxygen electrodes, Applied Catalysis B: Environmental. 182 (2016) 123–131. https://doi.org/https://doi.org/10.1016/j.apcatb.2015.09.011.

[19] M. Chandesris, V. Médeau, N. Guillet, S. Chelghoum, D. Thoby, F. Fouda-Onana, Membrane degradation in PEM water electrolyzer: Numerical modeling and experimental evidence of the influence of temperature and current density, International Journal of Hydrogen Energy. 40 (2015) 1353–1366. https://doi.org/10.1016/j.ijhydene.2014.11.111.

[20] I. Dedigama, P. Angeli, K. Ayers, J.B. Robinson, P.R. Shearing, D. Tsaoulidis, D.J.L. Brett, In situ diagnostic techniques for characterisation of polymer electrolyte membrane water electrolysers - Flow visualisation and electrochemical impedance spectroscopy, International Journal of Hydrogen Energy. 39 (2014) 4468–4482. https://doi.org/10.1016/j.ijhydene.2014.01.026.

[21] K. Elsøe, L. Grahl-Madsen, G.G. Scherer, J. Hjelm, M.B. Mogensen, Electrochemical Characterization of a PEMEC Using Impedance Spectroscopy, Journal of The Electrochemical Society. 164 (2017) F1419–F1426. https://doi.org/10.1149/2.0651713jes.

[22] P. Córdoba-Torres, T.J. Mesquita, O. Devos, B. Tribollet, V. Roche, R.P. Nogueira, On the intrinsic coupling between constant-phase element parameters α and Q in electrochemical impedance spectroscopy, Electrochimica Acta. 72 (2012) 172–178. https://doi.org/10.1016/j.electacta.2012.04.020.

[23] W. Sheng, H.A. Gasteiger, Y. Shao-Horn, Hydrogen Oxidation and Evolution Reaction Kinetics on Platinum: Acid vs Alkaline Electrolytes, Journal of The Electrochemical Society. 157 (2010) B1529. https://doi.org/10.1149/1.3483106.

[24] J. Rossmeisl, Z.W. Qu, H. Zhu, G.J. Kroes, J.K. Nørskov, Electrolysis of water on oxide surfaces, Journal of Electroanalytical Chemistry. 607 (2007) 83–89. https://doi.org/10.1016/j.jelechem.2006.11.008.

[25] S. Siracusano, S. Trocino, N. Briguglio, V. Baglio, A.S. Aricò, Electrochemical impedance spectroscopy as a diagnostic tool in polymer electrolyte membrane electrolysis, Materials. 11 (2018). https://doi.org/10.3390/ma11081368.

[26] C. Rozain, P. Millet, Electrochemical characterization of Polymer Electrolyte Membrane Water Electrolysis Cells, Electrochimica Acta. 131 (2014) 160–167. https://doi.org/10.1016/j.electacta.2014.01.099.

[27] J. van der Merwe, K. Uren, G. van Schoor, D. Bessarabov, Characterisation tools development for PEM electrolysers, International Journal of Hydrogen Energy. 39 (2014) 14212–14221. https://doi.org/10.1016/j.ijhydene.2014.02.096.

[28] A.M. Dhirde, S. Member, N. v Dale, H. Salehfar, S. Member, M.D. Mann, T.-H. Han, A.M. Dhirde, H. Salehfar, M.D. Mann, T. Han, Equivalent Electric Circuit Modeling and Performance Analysis of a PEM Fuel Cell Stack Using Impedance Spectroscopy, Ieee Transactions on Energy Conversion. 25 (2010) 778–786. https://doi.org/10.1109/TEC.2010.2049267.

[29] N. Ramaswamy, N. Hakim, S. Mukerjee, Degradation mechanism study of perfluorinated proton exchange membrane under fuel cell operating conditions, Electrochimica Acta. 53 (2008) 3279–3295. https://doi.org/https://doi.org/10.1016/j.electacta.2007.11.010.

[30] S.A. Grigoriev, K.A. Dzhus, D.G. Bessarabov, P. Millet, Failure of PEM water electrolysis cells: Case study involving anode dissolution and membrane thinning, International Journal of Hydrogen Energy. 39 (2014) 20440–20446. https://doi.org/10.1016/j.ijhydene.2014.05.043.

[31] T. Bystron, M. Vesely, M. Paidar, G. Papakonstantinou, K. Sundmacher, B. Bensmann, R. Hanke-Rauschenbach, K. Bouzek, Enhancing PEM water electrolysis efficiency by reducing the extent of Ti gas diffusion layer passivation, Journal of Applied Electrochemistry. 48 (2018) 713–723. https://doi.org/10.1007/s10800-018-1174-6.

[32] F. Fouda-Onana, M. Chandesris, V. Médeau, S. Chelghoum, D. Thoby, N. Guillet, Investigation on the degradation of MEAs for PEM water electrolysers part I: Effects of testing conditions on MEA performances and membrane properties, International Journal of Hydrogen Energy. 41 (2016) 16627–16636. https://doi.org/10.1016/j.ijhydene.2016.07.125.

[33] S. Sun, Y. Xiao, D. Liang, Z. Shao, H. Yu, M. Hou, B. Yi, Behaviors of a proton exchange membrane electrolyzer under water starvation, RSC Advances. 5 (2015) 14506–14513. https://doi.org/10.1039/c4ra14104k.

[34] J. Zhang, B.A. Litteer, W. Gu, H. Liu, H.A. Gasteiger, Effect of Hydrogen and Oxygen Partial Pressure on Pt Precipitation within the Membrane of PEMFCs, Journal of The Electrochemical Society. 154 (2007) B1006. https://doi.org/10.1149/1.2764240.

[35] P. Aßmann, A.S. Gago, P. Gazdzicki, K.A. Friedrich, M. Wark, Toward developing accelerated stress tests for proton exchange membrane electrolyzers, Current Opinion in Electrochemistry. 21 (2020) 225–233. https://doi.org/10.1016/j.coelec.2020.02.024.

[36] C. Wannek, B. Kohnen, H.F. Oetjen, H. Lippert, J. Mergel, Durability of ABPBI-based MEAs for high temperature PEMFCs at different operating conditions, Fuel Cells. 8 (2008) 87–95. https://doi.org/10.1002/fuce.200700059.

[37] S. Yu, L. Xiao, B.C. Benicewicz, Durability studies of PBI-based high temperature PEMFCs, Fuel Cells. 8 (2008) 165–174. https://doi.org/10.1002/fuce.200800024.

[38] D. Schonvogel, M. Rastedt, P. Wagner, M. Wark, A. Dyck, Impact of Accelerated Stress Tests on High Temperature PEMFC Degradation, Fuel Cells. 16 (2016) 480–489. https://doi.org/10.1002/fuce.201500160.

[39] P. Trinke, B. Bensmann, R. Hanke-Rauschenbach, Experimental evidence of increasing oxygen crossover with increasing current density during PEM water electrolysis, Electrochemistry Communications. 82 (2017) 98–102. https://doi.org/10.1016/j.elecom.2017.07.018.

[40] S.H. Frensch, G. Serre, F. Fouda-Onana, H.C. Jensen, M.L. Christensen, S.S. Araya, S.K. Kær, Impact of iron and hydrogen peroxide on membrane degradation for polymer electrolyte membrane water electrolysis: Computational and experimental investigation on fluoride emission, Journal of Power Sources. 420 (2019) 54–62. https://doi.org/10.1016/j.jpowsour.2019.02.076.